Title

The mechanisms responsible for 2-dimensional pattern formation in bacterial macrofiber populations grown on solid surfaces: fiber joining and the creation of exclusion zones

Journal

BMC Microbiology, 2(1)

ISSN

1471-2180

Authors

Mendelson, Neil H
Morales, David
Thwaites, John J

Publication Date

2002

DOI

10.1186/1471-2180-2-1

Peer reviewed

BMC Microbiology

Research article

The mechanisms responsible for 2-dimensional pattern formation in bacterial macrofiber populations grown on solid surfaces: fiber joining and the creation of exclusion zones

Neil H Mendelson*[1], David Morales[1,2] and John J Thwaites[3]

Address: [1]Department of Molecular and Cellular Biology, University of Arizona, Tucson, AZ 85721, [2]Department of Mathematics, University of Arizona, Tucson, AZ 85721 and [3]Gonville & Caius College, Cambridge, CB2 1TA, U.K

E-mail: Neil H Mendelson* - nhm@u.arizona.edu; David Morales - dmorale@u.arizona.edu; John J Thwaites - nhm@u.arizona.edu

*Corresponding author

Published: 28 January 2002

BMC Microbiology 2002, **2**:1

Received: 28 November 2001
Accepted: 28 January 2002

This article is available from: http://www.biomedcentral.com/1471-2180/2/1

Abstract

Background: When *Bacillus subtilis* is cultured in a complex fluid medium under conditions where cell separation is suppressed, populations of multicellular macrofibers arise that mature into ball-like structures. The final sedentary forms are found distributed in patterns on the floor of the growth chamber although individual cells have no flagellar-driven motility. The nature of the patterns and their mode of formation are described in this communication.

Results: Time-lapse video films reveal that fiber-fiber contact in high density populations of macrofibers resulted in their joining either by entwining or supercoiling. Joining led to the production of aggregate structures that eventually contained all of the fibers located in an initial area. Fibers were brought into contact by convection currents and motions associated with macrofiber self-assembly such as walking, pivoting and supercoiling. Large sedentary aggregate structures cleared surrounding areas of other structures by dragging them into the aggregate using supercoiling of extended fibers to power dragging. The spatial distribution of aggregate structures in 6 mature patterns containing a total of 637 structures was compared to that expected in random theoretical populations of the same size distributed in the same surface area. Observed and expected patterns differ significantly. The distances separating all nearest neighbors from one another in observed populations were also measured. The average distance obtained from 1451 measurements involving 519 structures was 0.73 cm. These spacings were achieved without the use of flagella or other conventional bacterial motility mechanisms. A simple mathematical model based upon joining of all structures within an area defined by the minimum observed distance between structures in populations explains the observed distributions very well.

Conclusions: Bacterial macrofibers are capable of colonizing a solid surface by forming large multicellular aggregate structures that are distributed in unique two-dimensional patterns. Cell growth geometry governs in an hierarchical way the formation of these patterns using forces associated with twisting and supercoiling to drive motions and the joining of structures together. Joining by entwining, supercoiling or dragging all require cell growth in a multicellular form, and all result in tightly fused aggregate structures.

Background

Cells of *Bacillus subtilis* grown under conditions where daughter cells fail to separate after each cell cycle, although the cytoplasm has been compartmentalized by septum formation, produce filaments consisting of chains of cells linked end to end [1]. Such filaments twist as they elongate, writhe, and eventually touch themselves. There follows a rapid winding up of the filament into a double-strand helix by a process of supercoiling that is triggered by the impediment of the twisting motions that accompany cell growth [2]. The cells in double-strand helical structures also twist as they grow. Their motions cause the double-strand structure itself to twist. Constraints on twisting again result in writhing, touching, and supercoiling. The product is a 4-strand helical structure [3,4]. A mature macrofiber arises by the repetition of the growth, twisting, and supercoiling process. The final structure is millimeters in length and contains tens to hundreds of cell filament strands twisted together into a coherent fiber with loops at both ends. The handedness of the initial double-strand helix is preserved throughout fiber morphogenesis suggesting that each cycle of supercoiling is a result of negative twist rather than simple over tightening of the previous helical form into a positive supercoil [5].

Macrofiber self-assembly ceases when structures become too stiff to supercoil into a plectoneme as a result of the number of cell filaments in the fiber shaft. Cell growth continues beyond this point however forcing the fiber shaft to supercoil into a free standing helix that contracts into a ball-like form [6]. Filaments that grow on the surface of a ball can buckle and initiate the outgrowth of fibers that remain anchored to the ball surface [7]. These too supercoil when they reach a critical length or when they encounter an external impediment to their twisting. In either case supercoiling draws an outgrowing fiber back onto the surface of the ball resulting in an expansion of it's diameter.

Macrofiber-producing cells of *Bacillus subtilis* are slightly denser than the complex fluid growth medium, TB, in which fibers are produced [8]. Lacking functional flagella they settle to the floor of the growth chamber and move as a result of growth or convection currents in the fluid. Growth with twisting is the predominant cause of motions that take place during macrofiber morphogenesis and the production of the two-dimensional patterns of larger structures described in this paper. Helix-hand specific pivoting motions of macrofibers and their walking over glass and plastic surfaces using forces generated by cell growth have been described previously [7,8]. These motions coupled with the joining of structures to one another upon contact govern the spacing distances between structures in a population situated on a solid surface. Unlike other spacing mechanisms found in procaryotes the macrofiber system appears to be a ramification solely of mechanics dictated by the organization of cells in multicellular structures and their growth geometry.

Results

Time-lapse video films of macrofiber populations grown as static cultures in 85 mm diameter plastic petri dishes containing 10 ml of TB medium were used to analyze the locations where structures were positioned on the floor of the petri dish, and the factors responsible for the patterns formed by them. The cultures studied were inoculated by sterile toothpick transfer from mature fibers grown in the same medium. A random number of fiber fragments was generated by the transfer process, each below the resolution of the optical system used to produce the films. These grew and self-assembled into macrofibers that could be seen distributed throughout the available surface area of the petri dish floor. When growth was allowed to continue undisturbed beyond the fiber stage the final populations contained 5 to 10 fold fewer multicellular structures than the number of fibers that could be visualized initially. Figure 1 illustrates that joining of fibers to one another was responsible for the reduction in their numbers, for the large increased mass of the final structures compared to the initial fibers, and for the eventual spatial pattern observed. In Figure 1 about 10 structures can be resolved at the earliest time shown [frame 1]. 167 minutes later [frame 16] only two multi-fiber structures remained in the same area. Additional file 1 shows the source film from which these frames were obtained. The growth rate of fibers in this culture measured by the rate of length increase was approximately 96 minutes per generation. A 5-fold reduction in the number of structures was achieved therefore in less than two cell generations. The results shown in Figure 1 suggest moreover that the scale of the final spatial pattern must be governed by initial fiber density in the population and the length to which fibers grow.

The joining of macrofibers to one another is a growth-dependent process driven by twist and supercoiling. It requires fiber-fiber contact that impedes the free twisting of one or both structures. Depending upon the geometry of the two structures that make contact and whether or not both ends of a given structure are prevented from rotating, contact results in either entwining of the two, or supercoiling that gives rise to a ball-like form consisting of both partners. Figure 2 illustrates the joining of two fiber fragments by the formation of a functional butt splice. The fragments shown are typical of those produced by toothpick transfer of a mature fiber into fresh medium. Individual cell filaments protruding from the ends of both fragment shafts became entwined with one-another. The newly spliced structure behaved as a single mechanical entity in all it's subsequent behavior, including an experimentally induced helix hand inversion during which all

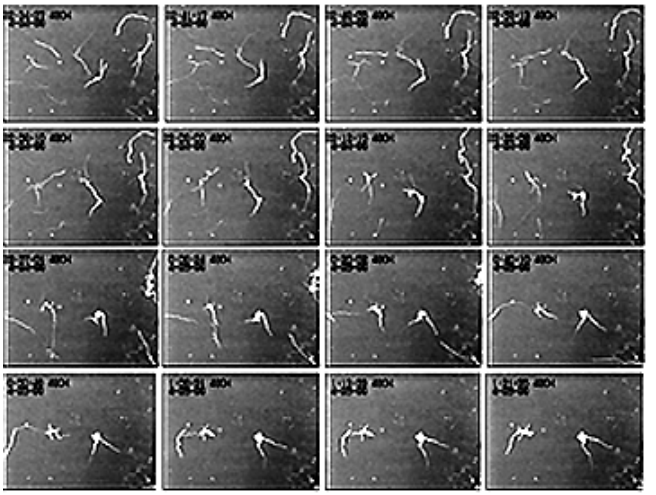

Figure 1
The joining of macrofibers to produce aggregate structures. 16 frames from film sequence 1 illustrate the joining of 10 right-handed FJ7 macrofibers to produce two aggregate structures. The time course of development was as follows: frame 1 = time 0. The following frames in order given in minutes after frame 1 = 6, 14, 18, 23, 28, 37, 48, 82,91,106,126,135, 154, 159, 167.

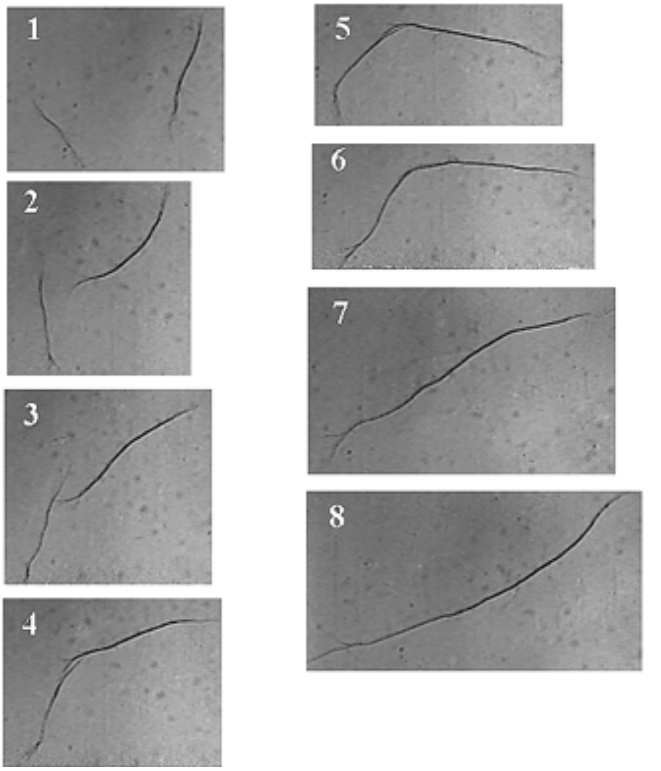

Figure 2
Butt splice formation of right-handed FJ7 macrofiber fragments. Eight frames from film sequence 2 show spontaneous end to end joining of fragments produced by entwining of cell filaments at their broken ends. Fragments no longer carrying terminal loops were produced by toothpick disruption of a parental fiber. Once joined the two fragments behaved as integrated components of a single fiber in terms of twisting, bending and writhing motions.

the cell filaments in the fiber's shaft unwound then twisted back together in the opposite helix hand. Additional file 2 shows the dynamics of splice formation and helix hand inversion. The maintenance of the splice throughout inversion illustrates that joining by entwining creates a strong linkage between the two entities. Joining by entwining also occurs when intact mature macrofibers with loops at their ends meet [9]. The resulting structures are irregular in diameter along their length reflecting differences in the diameter and/or topology of the two initial partners. Though irregular, joined structures of this sort are nevertheless mechanically sound and capable of continued self-assembly. They progress to mature ball-forms just as clonal fibers grown in isolation do.

Large and structurally complex macrofibers form ball-like structures rather than elongated ones as a result of supercoiling. Compare the geometry of forms in frames 1 and 16 of Figure 1. The ball-like forms produced by joining of large fibers are much more sedentary than their precursors. Figure 3 illustrates this. 10 large immobile structures are shown. The paths taken by precursor fibers leading to their contact and joining reveal the distances and directions travelled in the formation of each aggregate structure. For example, several of the initial 6 fibers that eventually became the one large ball-form aggregate shown on the upper left of Figure 3 traversed a distance of 5 mm from their initial positions to their final location in the aggregate structure. They moved over this distance either by "walking" over the plastic surface of the petri dish [10] until they met one-another, or by being "dragged" from one location to another as a result of supercoiling [11]. Structures too large to move themselves by walking can still be dragged from one location to another as shown in Figure 4 provided they acquire an extended fiber attached to their surface. In the case shown two structures too large to walk were drawn together by the supercoiling of an extended fiber that bridged between them. To begin with, the extended fiber had one free end capable of rotating as it grew. When rotation of the free end was prevented by contact with the second large ball structure supercoiling was induced. The two structures were then drawn together by the contraction in length that accompanies supercoiling. See Additional file 3 for an overview of the dragging process.

The static fluid cultures used in the experiments reported here always appear to develop internal fluid motions even

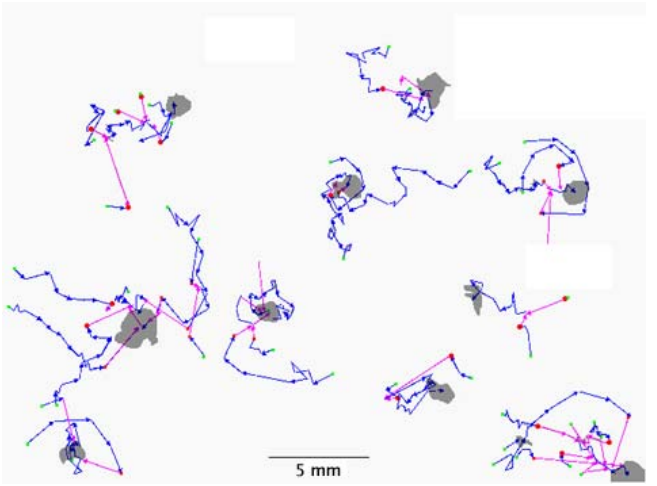

Figure 3
The paths travelled by FJ7 macrofibers during production of aggregate structures and pattern formation. Green dots represent starting positions of fibers. Orange dots mark the places to which fibers moved before making contact with another fiber. Blue lines depict the paths taken by walking, pivoting or supercoiling motions on the floor of the Petri dish. Pink lines show the paths taken during dragging motions. The grey blobs show locations and geometry of the final aggregate structures that form the pattern. The maps were produced by analysis of film sequence 3.

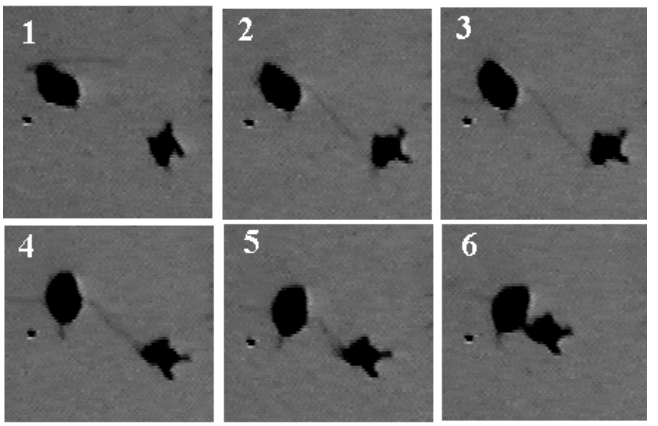

Figure 4
Dragging of two aggregate structures together by supercoiling of an extended fiber in contact with both. The images were taken from film sequence 1. A right-handed fiber attached to the surface of an aggregate structure swept clockwise around the aggregate from its point of attachment. In frame 3 it made contact with a neighboring structure, supercoiled in frames 4 to 6 and drew the neighboring structure to the surface of the initial structure to which it was connected. The two structures later fused together. This sequence illustrates the mechanism by which exclusion zones become established surrounding large structures.

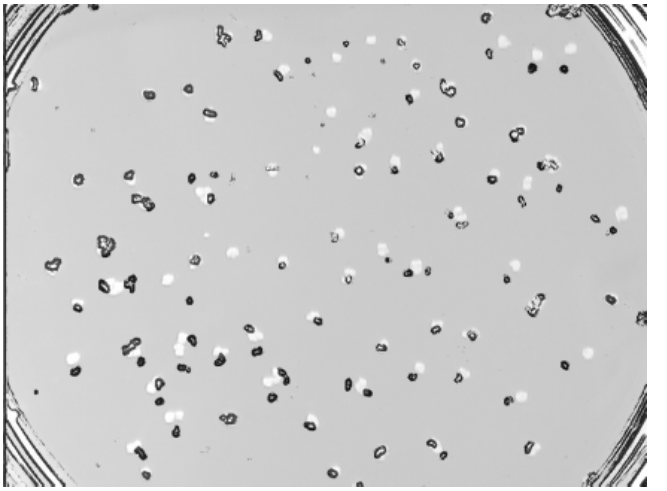

Figure 5
Motions of large structures late in pattern development. Two images from FJ7 macrofiber population 916 (frames 150 and 444) are superimposed upon one another and false colored black and white respectively. Parallel motions of structures in the same direction indicate the effect of convection currents. Time elapsed between the earlier and later frames was 441 minutes.

though the external environment is held at constant temperature. These convection currents can carry macrofibers with them, and can even move large ball-like structures. Figure 5 shows two frames taken from late stages of pattern formation in the same culture superimposed upon one-another. The structures in Figure 5 were false colored to permit identification of the earlier (black) and later (white) time points. A comparison of the two frames shows numerous examples of neighboring black structures joining to form a single white structure. The directions of the joining motions have no preferred orientation in the entire population. In contrast, comparison of the direction single black structures moved to their later white locations reveals that many paths taken are parallel to one another and in the same orientation. Smaller structures moreover moved over greater distances in the same time interval than did larger structures. Small structures of this sort are found in many cultures. They arise late in a culture's history apparently from filaments shed from large mature structures. Film sequences from other cultures show small late-arising structures moving over great distances amongst large structures that remain in place or move only very slightly. These observations indicate that convection currents must:

i. contribute to the motions fibers undergo in the early stages of pattern formation, and thus enhance the chances that fibers make contact with each other, and

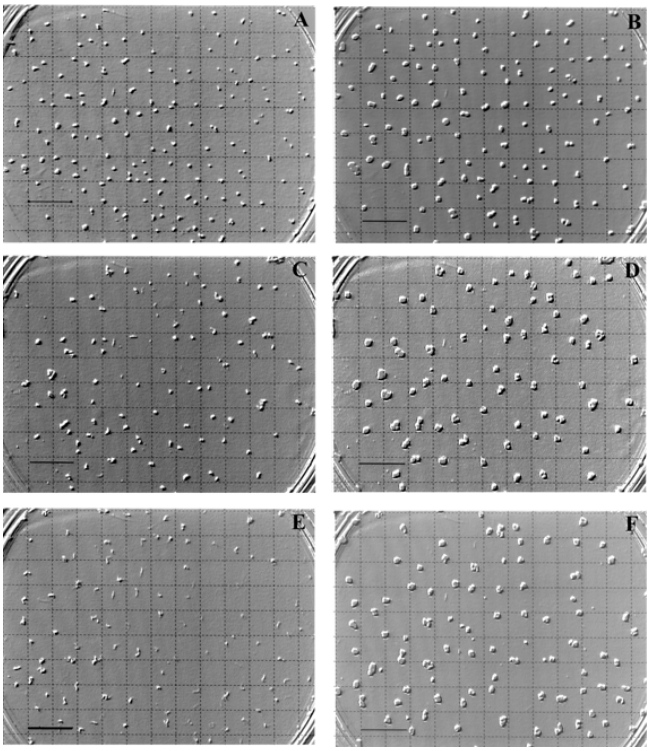

Figure 6
Images used to compare observed patterns of macrofiber aggregates with theoretical randomly distributed populations. Two video frames representing an earlier and later stage of pattern formation are shown for each of three FJ7 populations: A 97-frame 86, B 97-frame 142, C 916-frame 150, D 916-frame 444, E 920-frame 125, F 920-frame 400. Each grid square = 30.25 mm^2 of Petri dish surface. Bars = 10 mm. The filming rate was 1 frame/1.5 minutes.

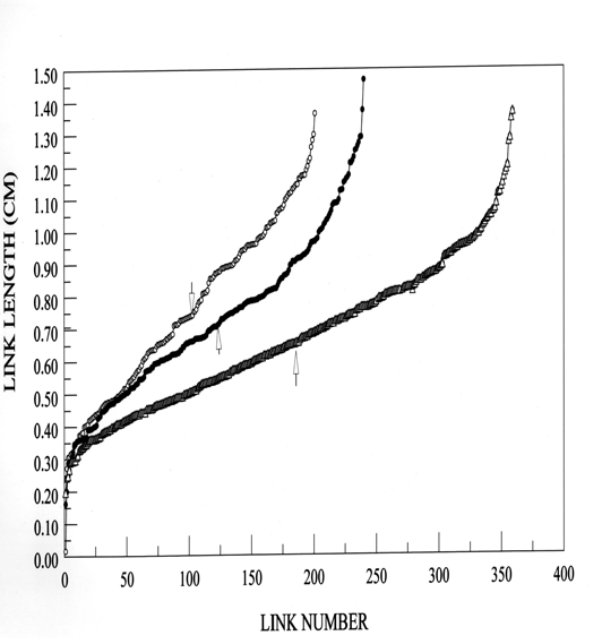

Figure 7
The lengths separating nearest neighbors in three populations of FJ7 macrofiber aggregate forms. All nearest neighbor links were drawn manually on images from populations 97–142, 916–444, and 920–400, and the length of each link was determined using a computer graphics program. The lengths were then ordered from shortest to longest within each population and plotted as a function of length. Arrows indicate the mean link length in each population. See Table 2 for further details.

ii. influence the final locations structures assume in the patterns.

The 2-dimensional spatial patterns of ball-form structures have been characterized in three macrofiber cultures designated 97, 916, and 920. Two time points were analysed from each culture: an early time when fibers were in the initial stages of ball formation but still capable of self-generated translational motions caused by twisting and supercoiling, and a later time when large ball forms were situated at or very close to their final positions. The six images analyzed are shown in Figure 6. In each pair of frames the total number of structures present at the later time is less than that present at the early time as a result of fiber joining. 637 structures are present in all six images. In order to determine whether structures are uniformly randomly distributed in the space available for each culture the observed distributions were compared to those expected on the basis of a Poisson distribution. A grid was superimposed over each image (Figure 6) and used to obtain the frequency of squares within which there were 0, 1, 2, or 3 structures. A Poisson distribution was used to predict the expected frequency for similar randomly distributed populations spaced uniformly in the same area. Both the observed and theoretical expected distributions are shown in Table 1. There are significantly fewer grid-squares that do not contain any structures in the observed populations than would be the case if the pattern was random. Similarly, there are more grid-squares that contain a single structure in the observed populations than would be anticipated if the structures were positioned solely by chance in the population. To validate the significance of these differences we performed a chi-squared comparison of the two populations (Table 1). They are significantly different and the χ^2 tests show that the probability of the observed distribution being uniform is very small.

The distances separating structures from all their nearest neighbors were determined in six populations. The results shown in Table 2 were derived from a total of 519 structures consisting of 1451 lengths measured between neighboring pairs of structures (called links). The mean

Table 1: Comparison of 2-dimensional spatial distributions of aggregate structures in observed and theoretical populations[1]

Population examined[6]	Number of structures	Number of squares	Average number of structures/ grid square[2]	Number of grid squares containing structures			
				0	1	2	3[5]
97–86[3]	154	103	1.50	15	40	38	10
expected[4]			1.50	23.1	34.5	25.8	12.9
97–142	115	104	1.11	19	57	26	2
expected			1.11	35.1	38.5	21.1	7.7
916–150	94	106	0.89	32	56	16	2
expected			0.89	43.7	38.7	17.2	5.1
916–444	74	106	0.70	45	49	11	1
expected			0.70	52.7	36.8	12.9	3.0
920–125	106	106	1.00	27	54	23	2
expected			1.00	39.0	39.0	19.5	6.5
920–400	94	106	0.89	36	47	22	1
expected			0.89	43.7	38.7	17.2	5.1

1. The populations shown in Figure 6 were used to obtain the observed values. **2.** The grid square area within which structures were counted was 30.25 mm^2. **3.** Two time points (frames) were measured from each sequence: 86 & 142, 150 & 144, 125 & 400. **4.** Expected values are Poisson distributions of theoretical populations with the same average number of structures per grid square. **5.** Squares containing 4 (1), 5 (2) and 6 (1) are included for population 97–86. **6.** Chi-square and p values were obtained by comparison of the observed and theoretical populations divided into 4 classes. Thus there are 3 degrees of freedom for all populations. The values obtained are: 97–86: 10.1, p = .017; 97–142: 21.6, p = .0001; 916–150: 12.8, p = .0048; 916–444: 6.8, p = .086; 920–125: 13.2, p = .0041; 920–400: 7.8, p = .052.

distances separating neighbors ranged from 0.65 to 0.85 cm in the five populations. The overall mean for all pairwise distances is 0.73 cm. The variation in separation distances within a given population can be examined by ordering all the separation distances in the network from shortest to longest and plotting them as a function of distance. Curves such as those shown in Figure 7 are obtained. The majority of points fall on straight lines the slopes and intercepts of which are given in Table 2. The separation distances between pairs become more uniform in populations with greater numbers of structures, as seen by the correlation between lower slopes and higher numbers of structures. A similar measurement of link lengths was carried out in theoretical populations distributed at random in the same space using a random number generator to assign x and y coordinates for each structure. Link lengths in these random populations also become more uniform as a function of object density in the population suggesting that improved uniformity of spacing in denser populations is not a ramification of the mechanism responsible for the patterns found in macrofiber populations.

The Y-intercept values listed in Table 2 represent the shortest distances separating structures in the observed populations. These values have been used in a model that predicts the observed distributions based upon the idea that all structures initially located within an area related to the Y-intercept value coalesce into a single structure. The following assumptions are made:

i. the starting structures are uniformly randomly distributed;

ii. a grid pattern with grid square size related to the Y-intercept value is superimposed upon the distribution of structures, these are termed "capture squares";

iii. all starting structures within each capture square coalesce, resulting in only two categories of grid squares: those with 0 and those with 1 structure in them.

For an initial average number of starting structures per capture square ν, the proportion of capture squares expected to contain 0 coalesced structures is (Poisson) $e^{-\nu}$, so that the proportion expected to contain 1 coalesced structure is $1 - e^{-\nu}$. Larger grid squares, termed "measuring grid squares" of any dimension can also be superimposed upon the same pattern of structures and the probabilities of finding r coalesced structures (r = 0,1,2, ... n) in the measuring squares that are n times as large as capture squares are, assuming that events in each capture square are independent of those in any other, given (Binomial) by:

$$P(r) = {}^{n}C_{r}p^{r}\,(1 - p)^{n-r}$$

Table 2: Spatial distributions of aggregate structures in populations

Population examined	Number of objects	Number[1] of links (cm)	Slope[2]	Y-intercept[2] (cm)	Mean link length (cm)
823[3]	48	143	0.0068	0.29	0.85 (0.78–0.94)[4]
916–444[5]	72	201	0.0042	0.32	0.75 (0.70–0.80)
920–400[5]	84	240	0.0027	0.37	0.72 (0.68–0.76)
812[6]	93	286	0.0031	0.28	0.75 (0.71–0.80)
916–150[5]	94	222	0.0043	0.32	0.65 (0.61–0.70)
97–142[5]	128	359	0.0018	0.33	0.65 (0.63–0.69)

1. The number of length measurements between all neighboring pairs of structures. 2. Determined from curves such as those shown in Figure 7. 3. Obtained by inoculating at four locations in the Petri dish rather than at random. 4. The values between which the mean link length will lie in 99% of populations. 5. Fiber fragments were dispersed by vortexing in 10 ml fresh TB prior to transfer. 6. Fiber fragments were transferred by toothpick directly from the parent culture.

where ${}^{n}C_{r}$ is the Binomial coefficient and $p = 1 - e^{-\nu}$

The expected average value for this distribution is $n(1 - e^{-\nu})$, called μ for simplicity. Using this average the probabilities for a measuring grid square 4 time larger than the capture square are:

$P(0) = (1 - 1/4\mu)^4$

$P(1) = \mu\ (1 - 1/4\mu)^3$

$P(2) = 3/8\ \mu^2(1 - 1/4\mu)^2$

$P(3) = 1/16\ \mu^2(1 - 1/4\mu)$

$P(4) = 1/256\ \mu^4$

Using population 97–86 as an example, the measured average is 1.4951. There are 154 structures and 103 measuring squares. The expected and observed frequencies of grid squares with 0 to 4 structures are as follows:

grid squares with	expected	observed
0 structures	15.8	15
1 structure	37.8	40
2 structures	33.9	38
3 structures	13.5	6
4 structures	2	1

The "fit" is clearly better than for a uniform theoretical distribution, but can be further improved by choosing a better ratio of measuring square area to capture square area. Table 3 shows the expected frequencies obtained when this model is applied to the six populations described in Table 1 with ratios either 3 or 2. No further attempt is made to optimize the fit, even so, the χ^2 probabilities show it to be very good. The ratios 3 and 2 correspond to the capture square sizes of 3.2 mm and 3.9 mm respectively. This range is almost exactly the same as that for minimum link distances for the cases in question (Table 2).

Discussion

The work described here focuses on the organization of multicellular bacterial forms in populations resting on a solid surface beneath a fluid growth solution. Although individual cells in these populations have no conventional mechanisms of motility their multicellular derivatives become dispersed in the space available forming patterns of unique scale and non-random character. Neither chemotactic processes, nor directed growth appear to be at play. Instead the ultimate patterns achieved are derived from the growth geometry of individual cells. Using the same basic mechanism that links cell growth geometry to macrofiber self-assembly we interpret the production of 2-dimensional pattern as an outcome of motions derived from cell growth operating at the level of a macrofiber and the joining of individual macrofibers to form higher order aggregates that have their own unique constraints. Both stochastic and determined events are involved. Unlike other bacterial populations in fluid cultures one ends up in the macrofiber system with condensed multiclonal structures of high cell density separated from one another according to rules based upon the ramifications of twisting and supercoiling of elastic filaments.

In macrofibers there is an hierarchical relationship between cell growth geometry, the behavior of cell filaments and bundles of filaments and the movement of macrofibers over solid surfaces. Individual cells, and consequently cell filaments also, twist as they elongate, encounter constraints on their twisting and supercoiling is an inevitable

Table 3: Comparison of observed and expected spatial distributions based upon the capture-zone model

Population examined		Ratio of measuring/ capture-zone square size[1]	Number of grid squares containing structures				Chi-square	
			0	1	2	3[3]		p
97–86	obs[2]	3	15	40	38	10	0.97	0.81 3 df[4]
	exp[2]		13.0	38.7	38.5	12.8		
97–142	obs	2	19	57	26	2	1.10	0.58 2 df
	exp		21.5	52.0	31.2	0		
916–150	obs	2	32	56	16	2	0.66	0.72 2 df
	exp		32.8	52.3	20.8	0		
916–444	obs	2	45	49	11	1	0.076	0.96 2 df
	exp		44.9	48.2	12.9	0		
920–125	obs	2	27	54	23	2	0.113	0.95 2 df
	exp		26.5	53.0	26.5	0		
920–400	obs	3	36	47	22	1	1.39	0.71 3 df
	exp		37.0	46.6	19.6	2.7		

1. The minimum link length (Y intercept from Table 2) from each population was used as as a guide to the length of a side of the capture zone square. The measuring square side length from Figure 6 was 5.5 mm for all populations. Ratios of 2 and 3 were chosen for illustration purposes with no attempt to optimize the fit to observed values. **2.** exp are values predicted by the capture zone model, obs are values from Table 1. **3.** Squares containing 4 (1), 5 (2) and 6 (1) are included for population 97–86. **4.** df are the degrees of freedom used to obtain the p values above them.

outcome. The mechanics of twisting elastic filaments assure self-assembly so long as the integrity of the cell filament, the backbone of cell wall peptidoglycan, and the electrostatic structure of the cell wall polymers is maintained. Fiber self-assembly has its limits however set by both physiological and mechanical constraints. There is a time course therefore when fibers are formed, mature, condense to ball-like forms and ultimately decay. Populations of fibers go beyond this clonal scenario by joining with one another and positioning the aggregate forms in patterns. Twisting and supercoiling are the key mechanisms responsible for these processes as well. In other words joining and positioning also require cell growth of a particular geometry.

Twisting motions enable macrofibers to join either by butt splicing or by parallel joining of two fiber shafts as a result of entwining. The case shown in Figure 2 illustrates that two different structures can join by entwining at the level of individual cell filaments in a manner similar to the early stages of clonal macrofiber formation. Supercoiling motions are responsible for:

i. fiber folding during morphogenesis [3]

ii. fiber movement over solid surfaces [7]

iii. the conversion of extended fibers into compact ball-form structures [11] and Figure 1

iv. the dragging of individual structures together which leads to their fusion into a aggregate multiclonal forms (Figure 4)

The cell surfaces that are brought into contact with one another by these processes show no signs of repulsion even when tightly pressed together by twisting and supercoiling, yet they do not bond together in a manner that prevents their sliding over one other during growth and movement. No obvious signs of attraction have been seen in many films examined that show pattern formation in populations. Nor is there any evidence that directed growth plays a role in bringing fibers close enough to each other for contact to be made. Rather it appears that random motions in high density populations position structures so that contact is inevitable as a result of growth motions. Once contact is made the laws of mechanics governing the behavior of twisting elastic filaments come into play and eventually a 2-dimensional pattern emerges (Figure 6).

Two features of the ultimate or penultimate 2-dimensional patterns formed by the positioning of ball-form macrofiber aggregate structures have been characterized here: their non-uniform randomness, and the spacing distributions of nearest neighbors. The former appears to be a ramification of the surface area within which fiber contacts can be made, itself governed by fiber length and fiber mobility. In late stages of pattern formation exclusion zones within which no other structures may exist become established surrounding each large structure. Any extended fiber that protrudes from the periphery of a large structure pivots about its anchor point as it grows and makes contact with the floor of the petri dish. The path travelled by the peripheral fiber(s) is governed by its helix hand (clockwise for right-handed, counter-clockwise for left-handed structures). The motion itself is caused by rolling and/or walking over the floor of the petri dish. During its sweep around the anchoring structure an extended peripheral fiber has the potential to drag any other structure it encounters to the surface of the anchoring structure thereby creating an exclusion zone. Exclusion zones are not perfect however. Peripheral fibers seldom sweep a full 360 degrees around a given structure before they either encounter another structure and supercoil pulling the two together or simply supercoil themselves onto the ball surface. Arcs may be left therefore that have not been cleared of neighbors. In addition peripheral fibers cease to function as a culture ages consequently a very late arising structure that happens into an exclusion zone can develop there into a mature structure. This is a very infrequent process however, easily detected in the film sequences, and did not occur during formation of any of the patterns analyzed here.

A mathematical model has been developed that predicts the two dimensional spatial distribution patterns of objects in populations that behave as macrofibers do. The key assumption is that all objects located within a capture zone join one another. Using minimum link lengths found in observed populations to scale the dimensions of the capture zone the model was able to predict distributions that closely match those found in the experimental populations (Table 3). These findings strengthen the contention that the condensation of macrofibers confined spatially into single aggregate structures is the essential mechanisms of pattern formation in macrofiber populations.

Finally mention must be made of the role convection currents play in the establishment of 2-dimensional patterns in populations. There is no question that convection currents move small and even large structures. In early stages of pattern formation when structures are very small and close to each other it is very likely that fluid flows do result in contacts that lead to joining. As structures grow larger and become multiclonal they no longer appear to be dominated by fluid currents and as their density in the population decreases chance positioning by convection becomes less likely. Walking, self-assembly motions, and supercoiling now dominate movements leading to chance contacts. Joining by dragging becomes the dominant mode at the latest stages of patterning. Eventually the density of objects in the population is at its lowest and the aggregate structures are very large, hence moved only slowly if at all by fluid motions. Once the culture reaches a stage where growth of individual cells is no longer in the organized fiber form, bringing structures together by any means is unlikely to result in their joining. The natural limit in pattern formation corresponds therefore to the time when there is no longer organized multicellular growth in the population.

Conclusions

Populations of bacterial macrofibers cultured in fluid medium without agitation produce aggregate multicellular structures distributed in 2-dimensional patterns on the floor of the growth chamber although the cells have no flagellar-driven motility. The geometry of individual cell growth is ultimately responsible for the observed patterns. Upon contact growing structures join one another using forces associated with twisting and supercoiling. The final result is a population of large sedentary aggregate structures separated from one another by surrounding zones of fluid medium that are free of structures. The scale of the pattern is set by the lengths to which mature macroflbers grow. A mathematical model based upon the coalescence of all structures initially located in proximity to each other is able to accurately predict the actual distributions found experimentally.

Materials and methods

Bacteria. *Bacillus subtilis* strain FJ7 has been described previously [15]. It may be grown as either left- or right-handed macroflbers with a range of twist states depending upon imposed environmental conditions. Young fibers produced in the standard complex medium, TB, were used as the starting material for all experiments.

Media and growth conditions. The complex medium, TB, consisted of 10 g Bacto Tryptose (Difco), 3 g Bacto Beef Extract (Difco) and 5 g NaCl per L deionized water. [15]. Static cultures were housed in standard 100 mm style diameter plastic Petri dishes (actual diameter of the floor = 85 mm). Right-handed fibers were produced by overnight growth in 10ml TB containing 50 mM $MgSO_4$ at 20°C. A single fiber was disrupted by toothpick transfer to fresh TB medium. Cultures grown for study at low magnification were placed on an elevated glass plate suspended above a black surface that was housed in a plexiglass chamber. The temperature on top of the glass plate was 24°C. Cultures used for higher magnification studies were grown on the stage of an Olympus SZ-Tr stereo zoom microscope housed in the same plexiglass chamber. Lighting was indirect from below using a source outside of the microscope to prevent temperatures from rising above 24°C. The culture from which Figure 2 was obtained was grown in TB medium lacking additional magnesium sulfate. It was incubated on the stage of a Nikon inverted phase contrast microscope and maintained at 48°C using an electrical heating/cooling device (Cambion, Cambridge Thermionic, Cambridge, MA).

Video film production and analysis. Time-lapse video films were produced at low magnification showing an entire Petri dish culture from above using a Cohu charged-coupled device camera fitted with a Fujinon TV zoom lens (1/12 175/75 mm) to which Tiffen closeup lenses were added as needed. Higher magnification films were obtained using either the stereo zoom microscope described above, or a Nikon inverted phase contrast microscope. Films obtained from the latter were initially recorded on 16 mm film using a Bolex camera controlled by a time-lapse system. The films were later transferred to VHS video format for analysis. All other films produced using Cohu cameras were recorded either with a GYYR time-lapse video VHS tape deck (Odetics) or a JVC time-lapse tape deck. In either case date and time stamps were written onto each frame by the tape deck. Images were transferred to a PC using Matrox software (Matrox Graphics, Montreal) and analyzed with Matrox and Image Pro Plus (Media Cybernetics) programs. The Adobe Photoshop program (Adobe Systems) was used to assemble the figures.

Additional material

Additional file 1

FJ7 macrofiber aggregate formation. A macrofiber population growing in fluid growth medium undergoes joining reactions to produce sedentary aggregate structures. The sequence is taken from a time-lapse film used to produce text Figure 1.
Click here for file
[http://www.biomedcentral.com/content/supplementary/1471-2180-2-1-S1.mov]

Additional file 2

Butt splice of macrofiber fragments. Two FJ7 macrofiber fragments are shown forming a butt splice upon contact while growing in fluid growth medium. The initial structures then undergo an experimentally induced helix hand reversal from right to left-handedness. The images shown in text Figure 2 were taken from this time-lapse film sequence.
Click here for file
[http://www.biomedcentral.com/content/supplementary/1471-2180-2-1-S2.mov]

Additional file 3

Motions of FJ7 macrofibers during pattern formation. A population of macrofibers growing in fluid growth medium is shown undergoing motions associated with their self-assembly and joining to form aggregate structures. Pivoting, walking, supercoiling and dragging motions can all be seen. The paths travelled during aggregate formation shown in text Figure 3 were taken from this time-lapse film.
Click here for file
[http://www.biomedcentral.com/content/supplementary/1471-2180-2-1-S3.mov]

Acknowledgements

This work was supported by a grant from the National Center for Research Resources, NIH to N.H.M. D.M was supported by the University of Arizona Undergraduate Biology Research Program. We thank J. C. Watkins for help with statistics, Darshan Roy and M. P. Finerty for technical assistance, and M. Wagenheim for processing video film images for internet use.

References

1. Mendelson NH: **Helical growth of *Bacillus subtilis* : a new model of cell growth.** *Proc. Natl. Acad. Sci. U.S.A.* 1976, **73**:1740-1744
2. Mendelson NH, Thwaites JJ, Kessler JO, Li C: **Mechanics of bacterial macrofiber initiation.** *J. Bacteriol.* 1995, **177**:7060-7069
3. Mendelson NH: **Self-assembly of bacterial macrofibers: a system based upon hierarchies of helices.** *Mat. Res. Soc. Symp. Proc.* 1992, **255**:43-54
4. Fein JE: **Helical growth and macrofiber formation in *Bacillus subtilis* 168 autolytic enzyme deficient mutants.** *Can J. Microbiol.* 1980, **26**:330-337
5. Mendelson NH: **Bacterial growth and division: genes, structures, forces and clocks.** *Microbiol. Rev.* 1982, **46**:341-375
6. Mendelson NH, Salhi B, Li C: **Physical and genetic consequences of multicellularity in *Bacillus subtilis*.** *In: Bacteria as Multicellular Organisms* 1997339-365
7. Mendelson NH, Sarlls JE, Thwaites JJ: **Motions caused by the growth of *Bacillus subtilis* macrofibres in fluid medium result in new forms of movement of the multicellular structure over solid surfaces.** *Microbiology.* 2001, **147**:929-937
8. Mendelson NH, Sarlls JE, Wolgemuth CW, Goldstein RE: **Chiral self-propulsion of growing bacterial macrofibers on a solid surface.** *Phys. Rev. Lett.* 2000, **84**:1627-1630
9. Mendelson NH: **Helical *Bacillus subtilis* macrofibers: morphogenesis of a bacterial multicellular macroorganism.** *Proc. Natl. Acad. Sci. USA* 1978, **75**:2478-2482

10. Mendelson NH: ***Bacillus subtilis* macrofibers, colonies and bioconvection patterns use different strategies to achieve multicellular organization.** *Environ. Microbiol.* 1999, **1**:471-477
11. Mendelson NH: **Dynamics of *Bacillus subtilis* helical macrfiber morphogenesis: writhing, folding, close packing, and contraction.** *J. Bacteriol.* 1982, **151**:438-449
12. Favre D, Mendelson NH, Thwaites JJ: **Relaxation motions induced in *Bacillus subtilis* macrofibres by cleavage of peptidoglycan.** *J. Gen. Microbiol.* 1986, **132**:2377-2385
13. Mendelson NH, Thwaites JJ, Favre D, Surana U, Briehl MM, Wolfe A: **Factors contributing to helical shape determination and maintenance in *Bacillus subtilis* macrofibers.** *Ann. Inst. Pasteur Microbiol.* 1985, **136A**:99-103
14. Mendelson NH: **The helix clock: a potential biomechanical cell cycle timer.** *J. Theor. Biol.* 1982, **94**:209-222
15. Mendelson NH, Favre D: **Regulation of *Bacillus subtilis* macrofiber twist development by ions: effects of magnesium and ammonium.** *J. Bacteriol.* 1987, **169**:519-525